

Volume III Update Report

Chapter 1

The ESS SC Reference Linac

Authors and Contributors

The ESS SC Reference Linac

Authors:

A Letchford,² K Bongardt³

Contributors:

B Aune,¹ P Y Beauvais,¹ R Bennett,² K Bongardt,³ W Bräutigam,³ M Desmons,¹ G Devanz,¹
R Duperrier,¹ R Ferdinand,¹ D Findlay,² I Gardner,² R. Gobin,¹ H Jones,² J L Laclare,¹
J M Lagniel,¹ A Letchford,² A Loulergue,¹ M Luong,¹ R Maier,³ S Martin,³ A Morris,²
A Mosnier,¹ M Pabst,³ M Painchault,¹ J Payet,¹ N Pichof,¹ C Prior,² G Rees,² Y Senichev,³
S Schriber,⁴ J Sherman,⁴ R Stassen,³ J Thomason,² D Uriot,¹ E Zaplatin³

¹CEA, ²RAL/ISIS, ³FZJ, ⁴LANL

Contents

The ESS SC Reference Linac

1	THE ESS SC REFERENCE LINAC	1-4
1.1	Overview	1-4
1.2	Introduction	1-4
1.3	The ESS SC REFERENCE LINAC	1-4
1.4	Linac front end	1-7
1.4.1	H ⁻ sources for the ESS SP&LP modes	1-8
1.4.2	The ESS chopper line	1-9
1.4.3	Particle Tracking along the ESS front end	1-11
1.4.4	RF systems for the ESS SC reference linac	1-13
1.5	1120 MHz ESS SC linac	1-14
1.5.1	Layout and parameters for the 1120 MHz ESS SC linac	1-15
1.4.5	Particle tracking along the ESS SC linac	1-17
1.4.6	RF control of the pulsed ESS SC cavities	1-20
1.5	Alternate ESS Scenarios	1-21
1.6	Status of the ESS accelerator system – the way ahead	1-23
1.7	Acknowledgements	1-23

1 THE ESS SC REFERENCE LINAC

1.1 OVERVIEW

This chapter describes the ESS Superconducting (SC) reference linac with its innovative chopper/collector system and the 1120 MHz high frequency SC part. At the presentation of the ESS project in the Former House of Parliament of the Federal Republic of Germany in Bonn, May 2002 the final decision on the accelerator technology (Normal or Superconducting) or frequencies had not yet been taken.

Results are presented for the chosen innovative chopper/collector system together with particle tracking along the ESS front end. Layout and parameters are shown for the ESS SC linac together with particle tracking up to ring injection point. The SC linac design is insensitive to different input distributions in spite of the 228 mA bunch current. Quite large RF amplitude & phase errors are tolerable here. Comments are given for a 2 msec H^+ linac feeding only the long pulse (LP) target, but with up to 15 MW beam power. Outlined are two dedicated test-stands necessary to construct the ESS facility within the new time schedule.

1.2 INTRODUCTION

The aim of the ESS project is to design an affordable, technically feasible next generation neutron source that on completion will provide World-leading performance for all classes of instrumentation. The result of a close dialogue between users, instrument designers, and target and accelerator experts is a facility with two complementary target stations. This is a **unique** feature of the ESS [Clausen, 2003]. The Long Pulse (LP) target station receives 5 MW of beam power from 2 ms long proton pulses with a frequency of $16\frac{2}{3}$ Hz (300 kJ/pulse). This is ideal for broad bandwidth applications where the integrated intensity is the important parameter. The Short Pulse (SP) target station also receives 5 MW of beam power but from 1.4 μ sec proton pulses arriving at a frequency of 50 Hz (100 kJ/pulse) for applications where the peak intensity in the pulse is the key parameter.

The high total beam power (10 MW), the demand for low loss in the accelerator and the combination of short and long pulses put rather stringent requirements on both the accelerator and the target stations. The proposed design, which either meets these requirements with currently available technology or where R&D activities have been outlined, has been scrutinised by an international group of leading experts and deemed feasible.

1.3 THE ESS SC REFERENCE LINAC

In the ESS technical proposal [ESS 2002] both NC (normal conducting) and SC (super conducting) solutions, with different frequencies, were described. All the described proposals were feasible and estimated to result in almost the same cost. A specific SC reference design has now been finally selected by the ESS accelerator team and approved by the ESS Council.

The layout of the accelerator system is shown in Figure 1.3.1, and the main parameters summarised in Table 1.3.1 About 10 MW operating power can be saved compared to ESS NC linac.

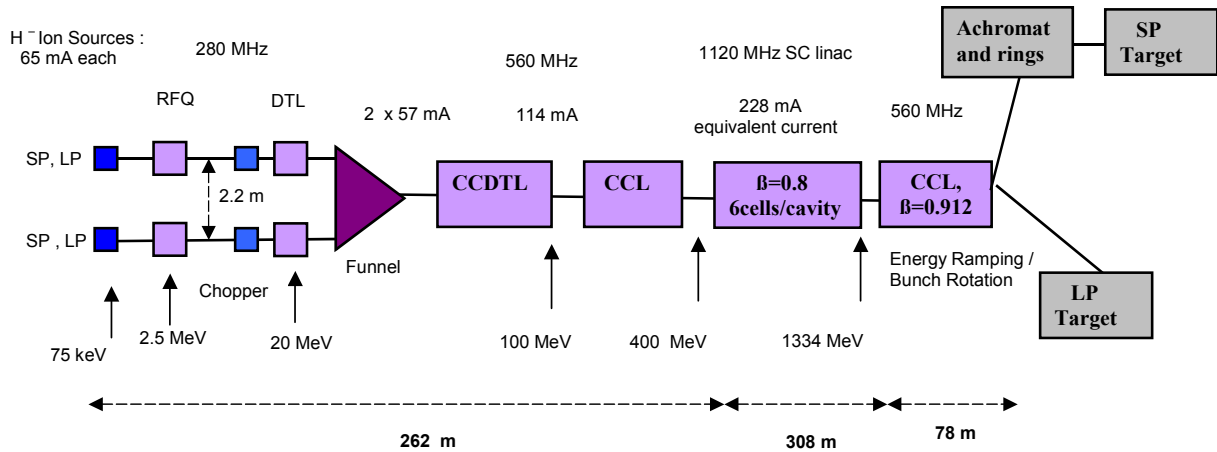


Figure 1.3.1: The ESS 1120 MHz Superconducting (SC) reference Linac

Table 1.3.1: Main parameters for the ESS reference linac with its simultaneous SP&LP operation. During commissioning the LP beam will also be chopped

	SP	LP
Beam Data		
PRF (pulses per second)	50	16.67
Beam pulse length(ms)	2x0.48	2.0
Beam duty factor	4.8%	3.3%
Non-chopped beam current (mA)	114	114
Chopping factor	70%	70% 100%
Final energy (MeV)	1334	1334
Peak beam power (MW)	107	107 152
Mean beam power (MW)	5.1	3.5 5.1
Pulse gaps, ring separation (ms)	0.1	
280/560 MHz NC-Linac		
Energy range (MeV)		400
NC linac length (m)		262
Peak RF power (nominal)(MW)	64	78 (100%)
RF pulse: length (msec) / duty cycle (d.c.)	1.4/7.0%	2.3/3.83%
Wall plug RF power (MW) (30 % RF control included)	12	8
1120 MHz SC-Linac		
Energy range (MeV)		400 –1334
SC linac length (m)		308
Accel. gradient in SC cells (MV/m)		10.2
Peak RF power (nominal) (MW)	75	107 (100 %)
RF pulse: length (ms) / d.c.	1.4/7.0%	2.3/3.83%
Wall plug RF power (MW) (30 / 40 % RF control included)	15 (40 %)	11 (30 %)
AC Cryo power (MW)	2.4	1.6

The main difference between the ESS accelerator and the accelerators currently under construction for SNS [SNS project] and J-PARC [Oyama, 2003] is the requirement of simultaneously delivering both short and long pulses [Clausen, 2003].

In order to deliver 5 MW beam power in about 1.4 μsec to the SP target, the ESS facility needs two accumulator rings with 35 m mean radius in a shared tunnel. Ring injection utilises H^- stripping injection with painting in the horizontal, vertical and momentum dimensions. Each ring is filled sequentially and injection is limited to 0.48 ms and 600 turns per ring in order to limit the temperature rise in each stripping foil, see chapter 3. The linac pulse is chopped to 70 % of the 800 ns ring revolution time at the ring revolution frequency to leave a gap for the ring extraction kicker magnets resulting in low ring losses. A 100 μs gap is required for vertical deflection of the linac beam between the rings. The pulse structure in the linac is shown in Figure 2. This makes the ESS facility **unique** in its neutron scattering performance, but is **challenging** for some ESS linac components: the front end with its chopping / collector system and layout / RF control of pulsed SC cavities.

The LP target station needs a 2 ms linac pulse every 60 ms or at 16.67 Hz repetition rate with 114 mA pulse current. This can be achieved with two H^- ion sources at 65 mA each, funnelled together at about 20 MeV. No beam chopping is required here, see Figure 1.3.2. The RF control system for pulsed SC cavities has to be very carefully designed as the system is matched only for the 2 msec un-chopped LP pulse, but quite heavily mismatched for the 70 % chopped SP. Operating at high frequencies and / or small accelerating gradients is a possible solution here.

The chopping line for the ESS linac must be able to switch the beam on and off between RF bunches resulting in elements with a rise time of less than 2 ns to avoid beam loss further down the accelerator. The beam collection system must be able to cope with up to 10 kW power, since both the SP and LP beam will be chopped initially.

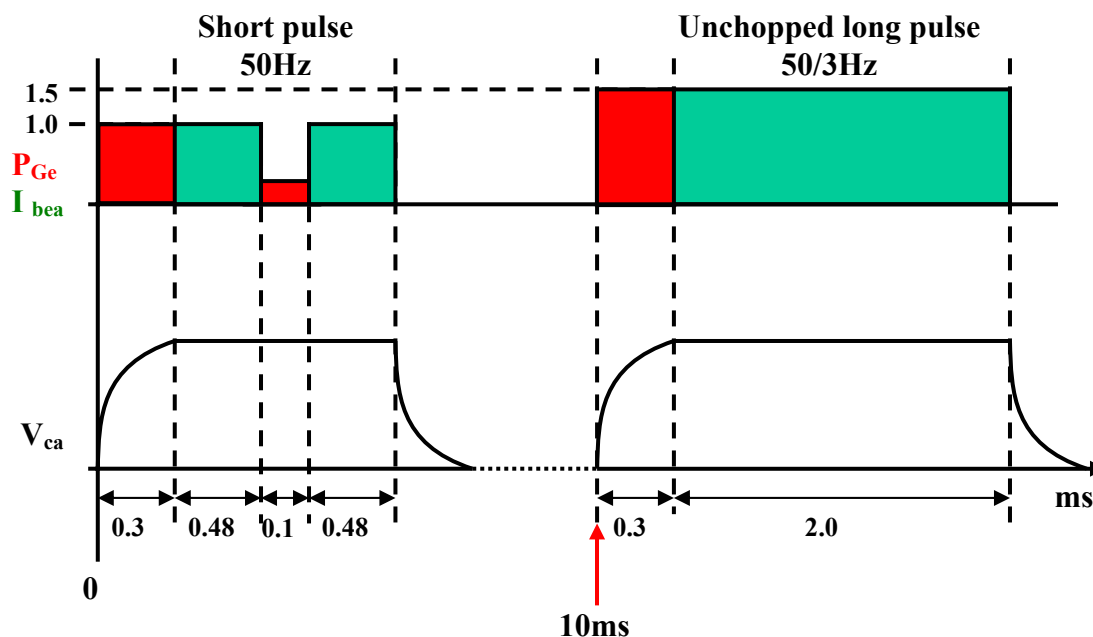


Figure 1.3.2: Pulse sequence on ESS linac, V_{ca} = Cavity voltage, I_{bea} = beam current relative to a chopped beam, P_{Ge} power from the RF generator for the SC cavities. Between the two ring pulses, the RF generator power has to be reduces to about 25 % in order to keep the accelerating voltage unchanged. **Not shown are the two other chopped pulses given to the SP target.**

The ESS reference linac with 10 MW of beam power, shared between the SP and the LP target stations, cannot be a direct copy of any current or planned linear accelerator. The ESS accelerator team therefore had to find a linac design that is cost effective and that will provide the 10 MW of beam power with a high degree of certainty. The 280 / 560 MHz normal conducting (NC) linac design described in ESS Volume 3 [ESS, 2002] is a technically feasible and physically robust design with a reasonable cost estimate. Selecting 1120 MHz elliptical SC cavities above 400 MeV and using the original 280 / 560 MHz NC linac below 400 MeV was found to promise both good beam quality with low losses and competitive construction and operating costs. The resulting main ESS linac parameters are shown in Table 1.3.1 and, as shown in Figure 1.3.1, the ESS reference linac starts with two parallel H^- beams, followed by a low frequency front end which houses an innovative chopper / collector system. Both H^- beams are combined at 20 MeV and accelerated in high frequency SC cavities from 400 MeV on. Placing 78 m behind the ESS linac NC $\beta = 0.91$, 560 MHz cavities for bunch rotation and 4 MeV energy ramping, see Figure 1.3.1, leads to a much easier RF control system than by using for SC cavities. The SP and LP beams are separated by 10 ms.

The 1120 MHz SC linac is 308 m in length and 172 cavities are required with only one SC main coupler per cavity designed for 0.85 MW peak power. Although cavity and cryostat can be scaled from the J-PARC 972 MHz SC proton linac test-stand, R&D is required for the SC main coupler. As the cavity bandwidth and stiffness is increased at the higher frequency, an 1120 MHz SC linac is well suited to guarantee loss free injection into both ESS compressor rings whilst not being hindered by the ESS SP & LP scheme.

To replace the warm parts of the ESS reference linac up to 400 MeV by SC low or medium β structures is not considered to be a valid alternative due to the ESS linac's RF duty cycle of only 12 % and the expected time scale for ESS, even if it is delayed by a few years. The ESS accelerator team regards SC low and medium β structures as an ongoing long-term R&D programme.

Operation of both long and short pulses may require two H^- ion sources in each leg of the front end. Neither the H^- ion-sources nor the chopper /collector system will be overloaded, but both beams must be combined at 20 MeV in the funnel. Progress in high intensity H^- ion-sources indicates that the ESS SP & LP requirements may be achieved with two H^- sources only, if the beams are separated by 10 ms.

1.4 LINAC FRONT END

The ESS front end part up to 20 MeV has been significantly improved compared to the description in ESS technical proposal [ESS, 2002]: Only one H^- source/ line is able to fulfil the SP & LP needs, which leads to a much more compact front end building and drastically simplifies the layout of the funnel section, as only $\pm 2^\circ$ final transverse deflection is needed, see chapter 6.2. We have now 4 instead of 2 fast deflectors in each chopper line allowing collecting all deflected bunches. The DTL up to 20 MeV uses an FFDD instead of an FD focusing scheme, which helps increasing the aperture radii. Particle tracking results are shown for the RFQ output distribution along the chopper section and the following DTL leading to very small filamentation afterwards. Particle loss in the chopper line is below 1 %.

1.4.1 H⁻ Sources for the ESS SP&LP modes

In ESS technical proposal [ESS, 2002] three H⁻ ion sources were considered as candidates for the ESS: the Rutherford Appleton Laboratory (RAL) ISIS surface Penning source, the Frankfurt volume source, and the Saclay ECR source. However most recent work has been carried out on the RAL Penning source, and it is a development of this source which will probably be used for the ESS, with the Frankfurt volume source, which has already achieved some of the ESS parameters, as a fall-back option. The Saclay ECR H⁻ source is too distant a possibility to be seriously considered for the ESS proposal [Gobin, 2002]. In Table 1.4.1 is presented a summary of the required parameters for the H⁻ ion sources, assuming a funnel is used.

Table 1.4.1: The Ion Source Parameters

Parameter	Short Pulses	Long Pulses
Ion current (mA)	65	65
Pulse length (ms)	2 × 0.48	2.0
Repetition rate (pps)	50	50/3
Duty factor (%)	4.8	3.3
Required lifetime	≥ 20 days	
Normalised emittance	≤ 0.3 π mm mrad	
Noise	≤ 2 % peak-to-peak	

The Penning source is being developed from the ISIS source currently in operation at RAL. The source is shown in cross section in Figure 1.4.1.1. The H⁻ beam is produced from a self-sustained plasma discharge in crossed electric and magnetic fields. It is a surface plasma source that produces H⁻ ions at the cathode surface of the discharge cell. Caesium is used to enhance the production of H⁻ ions by lowering the work function of the surface. In normal operation on ISIS the ion source operates at 35 mA during a 200 μs pulse at 50 pps, with normalised emittance ≤ 0.2 π mm mrad and an average lifetime of 26 days. The ESS front-end system is capable to handle such a small emittance, see section 1.4.3. Development work on the ISIS H⁻ surface Penning source to meet the duty factor and intensity requirements for the ESS has been carried out on an Ion Source Development Rig (ISDR) built for the purpose and funded by CCLRC¹ and the EU² [Thomason, 2002].

An H⁻ ion current of 65 mA will be achieved by increasing the potential of the ion source extraction electrode from 17 kV to 25 kV. A new 25 kV, 2 A, 3 ms pulsed power supply has been procured for this purpose, and a thorough examination of the electromagnetic fields in the extract electrode region has been undertaken using finite element analysis (FEA) software. Increasing pulse widths will necessitate an improved cooling system to offset increased heating. The optimal cooling strategy will be determined by thermal FEA, and may involve more aggressive cooling of the existing source or a scaling approach similar to that previously adopted on the 4X and 8X sources at Los Alamos [Sherman, 2002]. The mounting of

¹ Through the ISIS Department at RAL and CCLRC's Accelerator Science and Technology Centre (ASTeC).

² High Performance Negative Ion Sources Network, HPRI-CT2001-50021.

the development source has been modified to accommodate whichever approach proves most effective. The thermal model of the standard ISIS source is shown in Figure 1.4.1.1. Transient modelling suggests that the heating during a pulse decays rapidly into the thermal mass of the cathode when the pulse is switched off, and therefore it may be possible to derive long pulses at 50/3 pps interleaved with short pulses at 50 pps from the same ion source, provided that the further increase in heating can be dealt with.

A neutralized beam transport at 75 keV is foreseen in the LEBT, unchanged from the ESS technical proposal [ESS, 2002].

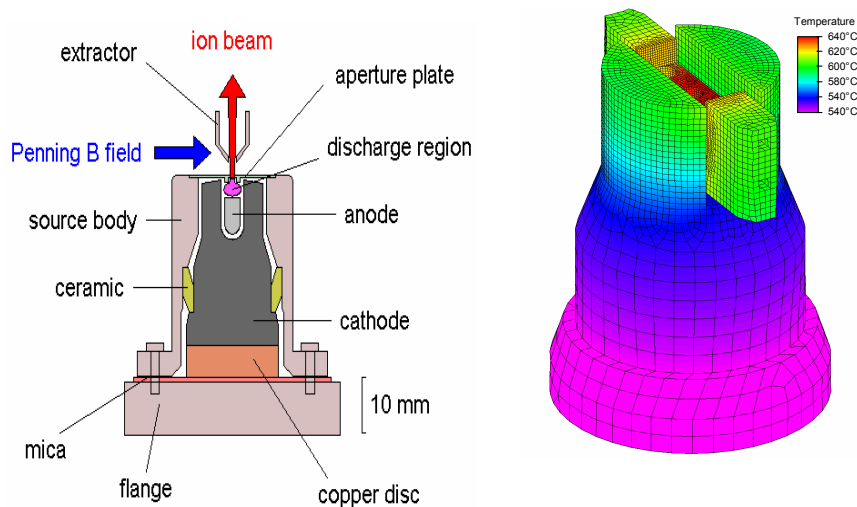


Figure 1.4.1.1: Schematic cross-section of the ISIS Penning H^- source and thermal model showing temperatures in the ion source anode and cathode

For ESS, an H^- volume source [Volk, 1998] has been developed and tested at the Institut für Angewandte Physik (IAP) in Frankfurt. The source consists of a caesium seeded multi-cusp plasma generator equipped with a variable filter magnet. Near the chamber axis, four tungsten filaments are mounted. Due to improvements of the caesium injection method, the beam current density was enhanced up to 153 mA/cm^2 . Thus, an H^- beam current of 120 mA was extracted using an emission opening radius of 5 mm. The required arc power for the production of this current was 50 kW. In operation with caesium, the e^-/H^- ratio is 6, whereas in operation without caesium the e^-/H^- ratio is between 50 and 100. The beam noise level is less than 1.5 % (peak-to-peak) and the lifetime of the ion source is about two weeks. The beam emittance has not yet been measured, but a rough estimation indicates an excellent beam quality. Operation of the source has been postponed because of safety regulations, but work has continued using computer modelling to optimise the electron dumping system.

1.4.2 The ESS chopper line

The 280 MHz low frequency front end houses the ESS chopper line with its 2 deflecting sections in order to collect up to 5 kW beam power in total at 4 different positions: the upper

and lower electrodes of chopper 2, Fig1.4.2.1. The 57 mA H^- bunch is kept focused in all three directions by using combined function elements between the deflectors. Focusing quadrupoles (Q) are incorporated into RF cavities(C). The complete chopper line from RFQ to DTL entrance is about 3.5 m in length.

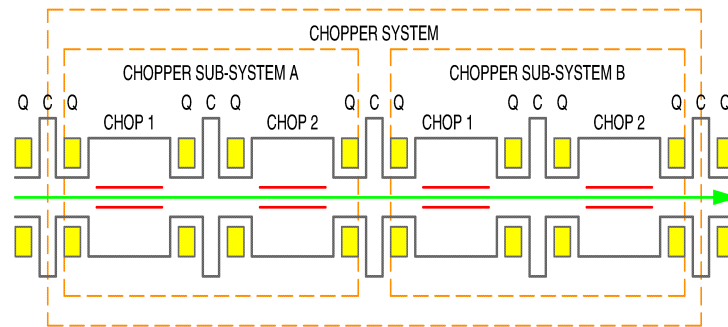


Figure 1.4.2.1: The ESS chopper line: 2 deflecting sections, 5 combined focusing elements

Each section consists of an innovative new chopper/collector system, where one chopper element ensures a fast rise time: ± 2 kV in 2 ns, 10 ns flat top. The other provides the long hold time for switching between the two rings and cleaning unwanted particles from the front end of the H^- pulse: ± 6 kV in 10 ns, with flat tops up to 100 μ s. The second chopper also acts as the beam collection system [Clarke-Gayther, 2002] for all deflected bunches, see Figure 1.4.2.2.

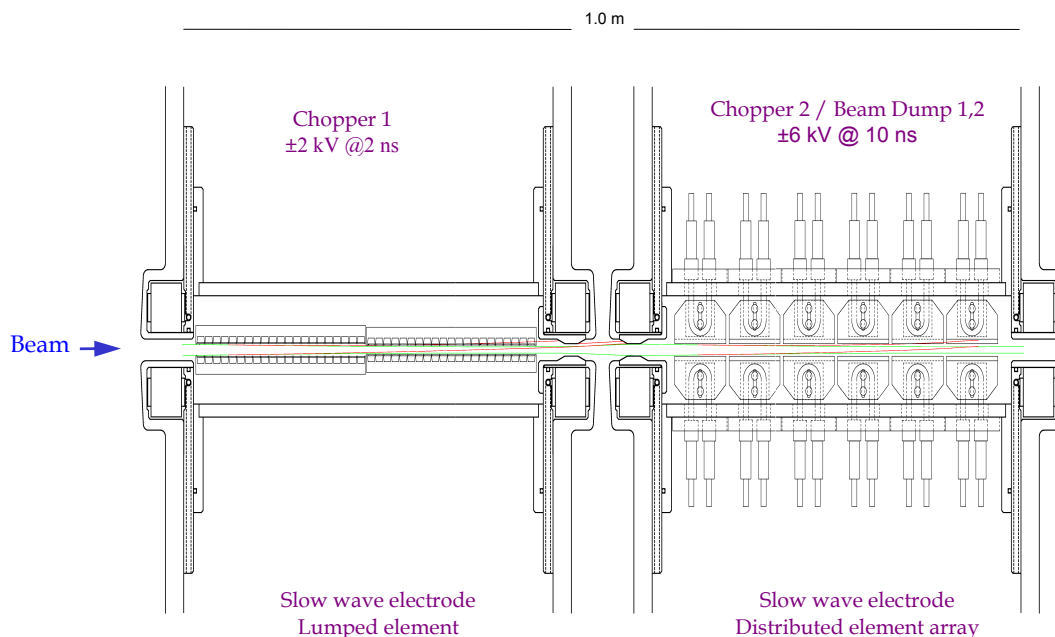


Figure1.4.2.2: The ESS chopper/collector system to achieve 2 ns rise time and 100 μ s flat top

As the ESS requirements on the front end systems are much more demanding than for the SNS and J-PARC facilities, a dedicated ESS front end test-stand must be built soon in order to start construction of the ESS facility in the medium term.

1.4.3 Particle tracking along the ESS front end

The DTL part between the chopper and the funnel section, see Figure 1.3.1, is a two tank Alvarez structure, with the first tank, DTL1, accelerating the beam from 2.493 to 11.4 MeV and the second, DTL2, continuing acceleration to 20.4 MeV. DTL1 and DTL2 have, respectively, 52 and 25 drift tube cells, and both are contained in a common vacuum tank to avoid a break in the focussing pattern. An alternative would be to have two separate tanks with a gap between, but with some cells in the transition region shifted in position to reduce the gap mismatch by changing the phase and hence the effect of the RF fields. Suitable tank spacing for this option is $1\beta\lambda$ as this preserves the transverse focussing structure. The initial option of a common vacuum tank for DTL1 and DTL2 is preferred, and the required tank length is then approximately 11 m.

An FFDD focussing scheme is chosen [Gerigk, 2003/1] which provides the same transverse focussing constants than the traditional FD focussing but with lower quadrupole gradients. Thus the bore radius can be increased providing a higher safety margin between the r.m.s. beam size and the pipe radius (6.5 instead of 4.5 as in the ESS Technical Report). Furthermore the tolerances on the quadrupole field alignment can be relaxed. The lower shunt impedance of this structure is counterbalanced by a slightly lower field level in the tanks, yielding 11 m of total DTL length instead of 9.5 m for the previous version. The RF design was made with the SUPERFISH [Billen, 2002] wrapper DTL_GEN [Uriot]. Adjustable electromagnetic quadrupoles are foreseen, following the design for the JHF-JAERI linac [Yoshino, 2000]. Additional steering coils are added to some quadrupole cores to allow H^- beam orbit correction. R & D is required for the design of this quadrupole.

The values of radii selected for the tank, the drift tubes and the bore are 570, 85 and 11 mm, respectively, and, for the β range 0.07 to 0.2, the transit time factors increase from 0.80 to 0.93 and the shunt impedances from 20.5 to 34.1 M Ω /m (SUPERFISH - 15 %). Two linear quadrupole gradient ramps are used in each tank, with values of 46.5 and 38.5 T/m at the input and output quadrupoles of DTL1 and with values of 31.0 and 27.0 T/m at the input and output of DTL2. The effective quadrupole length is increased from 40 mm in DTL1 to 52 mm in DTL2.

The Kilpatrick level in the tanks is kept constant at 1.3. Both tanks deliver approximately 60% of their 1.1 MW input power to the LP beam, see section 1.4.4. Adding 30% control power the klystrons each have to provide 1.33 MW of RF power, see Tab1.4.4.1. Post couplers are used for field stabilization in the tanks.

A linear ramp throughout DTL1 and DTL2 raises the electric field from 1.8 up to 2.47 MV/m while the synchronous phase is ramped from -42° to -30° . The longitudinal phase advance per period decreases from initially 30° to 16° at the linac end, while the transverse phase advance ranges from 35° to 28° . The longitudinal and transverse focussing is adjusted to keep the ratio of longitudinal over transverse phase advance below 0.8 in order to minimize emittance exchange between the planes.

Figure 1.4.3.1 show the r.m.s. beam radii and emittances evolution for a beam that was tracked from the RFQ input to the end of DTL2 using IMPACT [Qiang, 2000]. RFQ layout and resulting beam distributions are unchanged from the ESS technical proposal. Clearly can be seen the 4 chopper sections which its larger beam radii compared to the following DTL.

Longitudinal focusing in the chopper line is provided by 5 RF cavities / line, see Fig1.4.2.1, which keeps the r.m.s. phase width between 17° (1st cavity) and 12° (5th cavity). The ESS front-end system is capable to handle transverse r.m.s. emittances around 0.2π mm mrad, which helps reducing particle loss afterwards.

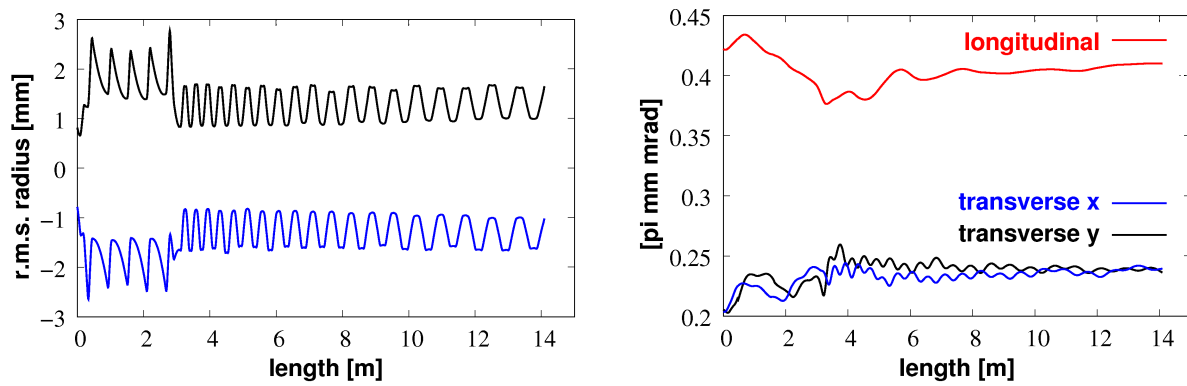


Figure1.4.3.1: Transverse r.m.s. beam radius (left) and r.m.s. emittances (right) along chopper line (up to 3.5 m) and DTL

Figure 1.4.3.2 shows the resulting phase space plots at the end of the DTL. Only little filamentation is visible, including the longitudinal plane. This allows doubling the frequency afterwards in the SC cavities.

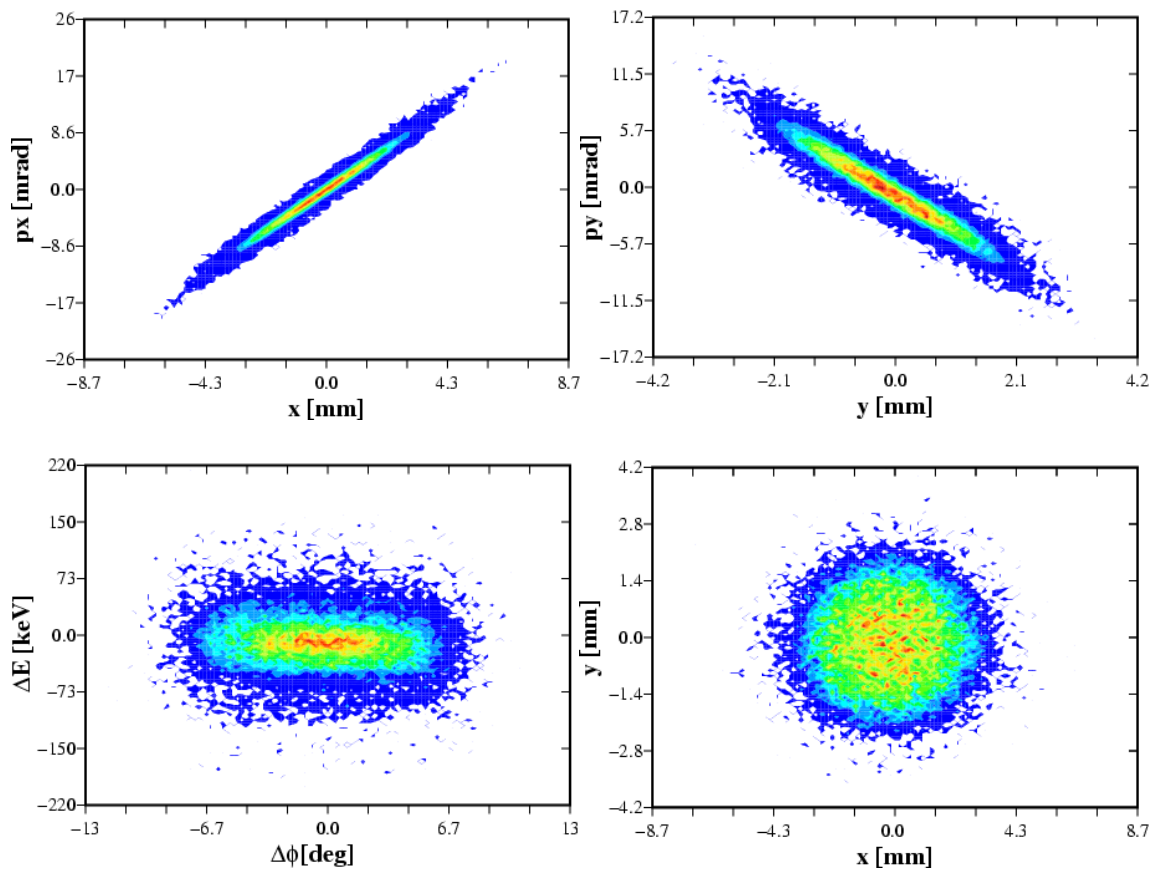


Figure1.4.3.2: Phase space at the output of the DTL (tracking from RFQ input)

Loss studies [Gerigk, 2003/1] suggest that due to the new aperture statistical errors (quadrupole, RF phase & energy) will not result in any beam loss in the DTL. Large amplitude halo particles from the RFQ are scraped in the chopper line. Particle loss here is below 1 % for a matched beam injected into the RFQ. The r.m.s. emittance increase for realistic statistical errors (max. static RF errors < 1 %, 1°, max. dynamic RF errors < 1 %, max. quadrupole gradient error < 0.5 %) is below 10 % in each plane [Gerigk, 2003/2]. The main concern, however, are partly filled displaced bunches from the chopper, RF phase & energy jitter, and increased error margins for the first bunches of each pulse due to ringing of the power supplies. First simulations are indicating much smaller energy, phase deviation of the beam at 20 MeV than used for the particle tracking along the SC linac, see section 1.5.2.

1.4.4 RF systems for the ESS SC reference linac

The RF system for the NC part of the ESS linac up to 400 MeV, see Figure 1.3.1, are medium or high power RF amplifier sets providing RF power outputs between ~30 kW and ~5 MW and at 280 respectively 560 MHz in the accelerating sections. For the 20 MeV funnel line, unchanged from the ESS technical proposal, same RF cavities operate at 840 MHz. The 280 MHz RFQ design as well as both 560 MHz accelerating sections are unchanged. As shown in Fig 1.3.1, a 560 MHz, $\beta = 0.912$ CCL section for bunch rotation (BR) is placed 78 m behind the linac end in order to reduce the energy spread and to slowly ramp up the beam energy by about 4 MeV, necessary to achieve loss free ring injection. In the NC part of the ESS linac, the difference in RF peak power is less than 30 % between the SP and the LP mode which allows using the same power supply for both operating modes. The main RF parameters for the ESS reference linac are shown in Table 1.4.2 for the LP mode with its 114 mA pulse current.

Table 1.4.2: RF parameters of the ESS 1120 MHz SC reference linac

Accelerator structure	Freq. (MHz)	Peak powers(nominal) (MW) (100 % chopped beam)			Number of klystrons & Peak power(with RF control)
		Structure	Beam	Total	
2 × RFQ	280	1.6	0.45	2.1	2 × 1.3 MW
2 × Chopper	280	0.15	~ 0	0.15	10 × ~ 0.04 MW
2 × DTL	280	1.3	2.0	3.3	4 × 1.3 MW
Funnel	840/ 560/280	0.7	~ 0	0.7	12 × ~ 0.08 MW
CCDTL	560	5	9	14	15 × 1.3 MW
CCL	560	22	35	57	22 × 5 MW
SCL	1120	~ 0	107	~ 107	172 × 0.85 MW
BR cavity	560	0.6	0.46	1.10	1x1.45 MW
Σ		~ 31	152	~ 185	238

To maintain the required phase relationships within accelerating cavities, the amplifier sets are all driven from one common source of RF, a master oscillator with an output of ~1 W³.

³ 1 W into 50 Ω corresponds to a (peak) amplitude of 10 V. If the RF level is much less than this it may be vulnerable to interference from noise and pick-up.

Three different harmonically related RF frequencies are required, and are obtained from the master oscillator by frequency multiplication and/or division. Each amplifier set is located as close as reasonably possible to the cavity(ies) it drives, and so inevitably the sets are spread over several hundred metres. CW RF is expected to be distributed⁴ at ~10 kW by waveguide, -40 dB couplers being used to feed the amplifier sets with ~1 W each. Each amplifier set is expected to be self-contained and to consist of a low power RF system, an intermediate stage driver amplifier, a final stage high power amplifier, a modulator, a power supply, an output feeder system, a cooling system, and a sophisticated control and monitoring system.

The choice of tube type for a final stage high power amplifier delivering ≥ 1 MW is almost certain to be the klystron⁵. The only possible exception might be at frequencies < 300 MHz, where the tetrode might be usable. At lower powers, the IOT (inductive output tube) is a possible useful alternative, as it is more efficient than the klystron and does not need a high power modulator. Both klystrons for the present application which have gains of 40–50 dB, and present-day IOTs which have gains of 20–25 dB and can deliver powers up to ~100 kW, can be driven by commercially available solid state RF amplifiers. The low power RF system would run at the ~1 W level, and would provide the following functions: RF phase and amplitude stabilisation to within $\pm 1\%$ and $\pm 1^\circ$ respectively⁶; fast inhibit for personnel safety and plant safety; frequency tuning control of the accelerating cavity(ies)⁷.

It is evident from previous sections of this chapter that some two hundred RF systems are required to drive the ESS linac. This is a large number, and so issues of reliability and resources must be specifically addressed. Consequently, there must be at least one off-line test bed for *each* of *all* the major RF components, *including* accelerating cavities. In addition, suitable numbers of spare components must be held, including klystrons, modulators, circulators, RF loads, intermediate stage amplifiers, low power modules, *etc.* Facilities must be provided for maintaining the spares in a proven operational condition⁸.

1.5 1120 MHz ESS SC LINAC

Above 400 MeV, 1120 MHz SC cavities accelerate the ESS beam up to its full 1334 MeV final energy. SC structures offer a reduction in operating costs compared to warm NC ones, but it requires a careful look at the pulsed RF control system especially for combined SP&LP requirements. Higher frequency SC structures are beneficial for the demanding ESS requirements and offer headroom for capital cost saving. As the ESS front end prefers low frequencies, a change in frequency from 560 MHz to 1120 MHz at 400 MeV is foreseen for the ESS reference linac.

⁴ The temperature of the waveguide may have to be closely controlled, as a temperature change of 5°C over 200 m is equivalent to 7° of phase at 560 MHz (for a coefficient of thermal expansion of 10^{-5}).

⁵ To prevent damage to klystrons RF output windows caused by excessive reverse RF power, circulators backed up by reverse power detectors and waveguide arc detectors would be used.

⁶ These limits are set primarily by beam requirements at injection into the accumulator rings and the need to minimise induction of radioactivity due to beam loss, and are not easy to meet.

⁷ The tuning of the cavities will be effected by varying the temperature of the cavity cooling water which must be reproducible to within $\pm 0.1^\circ\text{C}$.

⁸ For example, periodically spare klystrons should be powered up to confirm their performance.

1.5.1 Layout and parameters for the 1120 MHz ESS SC linac

The SC part of the linac uses 43 cryo-modules, each housing 4 elliptical bulk Nb SC cavities. Each cavity consists of 6 cells of $\beta=0.8$ equipped with one SC main coupler. Doublets in the warm intersections provide the transverse focusing, see Figure 1.5.1.1. The main parameters of the ESS SC linac are shown in Table 1.5.1 together with comments what has been achieved up to now for high frequency SC equipment.

The ESS cryomodule layout profits considerably from the work of the J-PARC team on their 972 MHz SC cavities. As the overall RF duty cycle is about 11%, we limited ourselves to only 0.85 MW peak power for the unchopped LP beam, leading to 80 kW SP&LP averaged power. Only 10 MV/m accelerating gradient at $Q_0 = 10^{10}$ is required, keeping the peak magnetic field well below 50 mT and leading to a matched cavity bandwidth of ± 2 kHz for the 114 mA LP beam. Cavity stiffening methods for reducing the Lorentz force frequency detuning are under investigation, absolutely necessary even for the envisaged 10 MV/m accelerating gradient due to the ESS SP&LP modes, see section 1.5.3. Under construction are SC main couplers at 1300 MHz, designed for either 1 MW peak [TESLA project], but with less than 1 % d.c. or for 100 kW CW power [ERL project].

About 5 kW cryo-power at 2 K equivalent is required for the ESS SC linac, 50 % more than for the SNS SC linac. The static loss is dominated by the cavities, the dynamic loss by the power couplers, where we used scaled values from the thermal analysis of the CW APT 420kW coupler [Bourque, 2001].

Klystrons at 928 MHz are commercial available with 1.3 MW peak power and 10 % d.c. for 2 ms long pulses. Combined High Voltage Power Supplies (HVPS) with common energy storage and pulse transformers, but different bouncer circuits and reset loops, are considered for SP&LP operation in order to be perveance matched on the klystron side [Bothe, 1996]. Central energy storage and control systems for a large number of klystrons are under investigations.

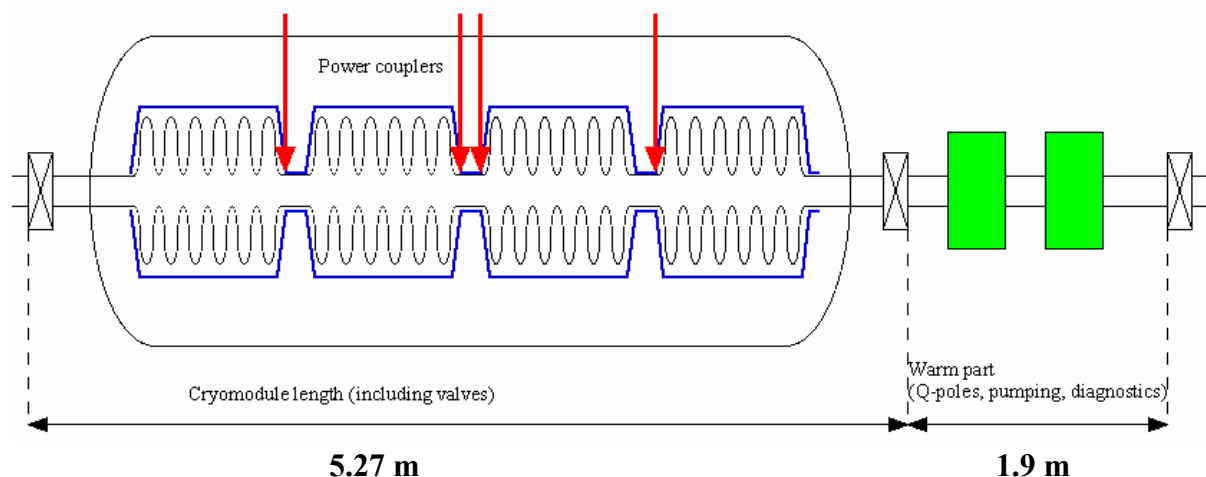


Figure 1.5.1.1: Schematic drawing of a lattice period of the SC linac

The klystron gallery for housing four klystrons & wave guides every 7.2 m is about 14m wide compared 10m in the NC part, unchanged from the ESS technical proposal, in order to shield the klystron from neutrons, generated by beam loss. The height of 6 m is the same for the NC and SC part. The accelerator tunnel itself is the same as for the NC part, unchanged from the ESS technical proposal [ESS 2002].

Higher gradients in the ESS SC linac are not in general excluded, but potential problems to be addressed are the SC main coupler and the pulsed RF control system under the ESS SP&LP conditions.

Table1.5.1: Main parameters of the ESS 1120 MHz SC linac

	technical data	comments
Cavity data : 172 cavities	<ul style="list-style-type: none"> • elliptical SC cavity, $\beta=0.8$ • 6 cells • 4 cm iris radius • 5 cm coupler port radius • acc.gradient 10.2 MV/m OR : peak surface gradient ~ 24 MV/m	<ul style="list-style-type: none"> • J-PARC SC linac : - 972 MHz , $\beta=0.75$, 9 cell - 6 cm iris radius & coupler port radius • $\beta=1$, 1.3 GHz TESLA elliptical SC cavities : > 60 MV/m peak surface gradient
Cryomodule : 43 cryomodules	<ul style="list-style-type: none"> • 4 cavities / module • 0.7 m cavity-cavity separation • total length of 5.27 m • 2 K operation 	<ul style="list-style-type: none"> • J-PARC SC linac : complete design of cryomodule • TESLA : - up to 9 cavities in one cryomodule - shielding at 4 K & 70 K
Focusing periode : L-per = 7.17 m L-SC = 308 m	<ul style="list-style-type: none"> • 1.9 m warm intersection • quads : 4 cm aperture radius 30 cm length, 14 T/m gradient 	
SC main coupler : - 1 coupler/cavity - 5 MW SP & 5 MW @ 2 msec to LP	<ul style="list-style-type: none"> • 0.85 MW peak power & 0.08 MW average power : cold coaxial line with about 5 cm radius 	<ul style="list-style-type: none"> • TTF IV coupler : 1 MW peak & 1.3 GHz • Cornell ERL coupler : 0.1 MW average & 1.3 GHz
Cryoplant: 5.1 kW at 2K equivalent , ≈ 4 MW AC power	<ul style="list-style-type: none"> • average heat load: 5.5 W/cavity • average load: 12 W/coupler • total section load : 3010 W 	<ul style="list-style-type: none"> • SNS medium β cryomodule with 3 cavities : measured static load of 17 W
1120 MHz RF system	<ul style="list-style-type: none"> • LP target : 0.85 MW peak, 2.3 msec every 60 msec • SP target: 0.65 MW peak, 1.5 msec every 20 msec • Klystron - NO modulating anode - $> 60\%$ DC to RF efficiency - cathode voltage ~ 92 KV 	<ul style="list-style-type: none"> • 928 MHz Thales TH 2162 : 1.3 MW peak, 2 msec, 10% d.c • for high efficient klystrons : product of $V * \tau^{0.5} = \text{con}$ 120 kV & 2 msec (1.3 GHz)
Surplus on RF power : (30 % , 40 %) for (LP,SP)	<ul style="list-style-type: none"> • 3 db cavity bandwidth of ± 2.0 kHz • LP mode operation : - reflection due to coupler tolerances - wave guide losses & RF control • in addition for SP mode : mismatch 	large bandwidth & small Lorentz detuning , but CHALLENGING for the ESS SP&LP modes
AC power supply	<ul style="list-style-type: none"> • combined LP/SP power supply , perveance matched at the klystron side : $> 80\%$ AC to DC efficiency 	various possibilities like the TESLA ones : - common energy storage - 2 separated LP/SP bouncers - common pulse transformer

1.4.5 Particle tracking along the ESS SC linac

Detailed Monte Carlo simulations with complete 3d space charge have been performed to demonstrate the capability of the 1120 MHz ESS SC linac to handle the 228 mA bunch current (114 mA pulse current) from 400 MeV onwards by using $\beta=0.8$, 6 cell cavities only [Pabst, 2002,2003]. Figure 1.5.2.1 shows the phase slip of the bunch centre for each cell of the total 172 cavities. The energy gain is changing from cell to cell, but stable synchrotron oscillation result, leading to acceptable longitudinal filamentation at the ESS linac end.

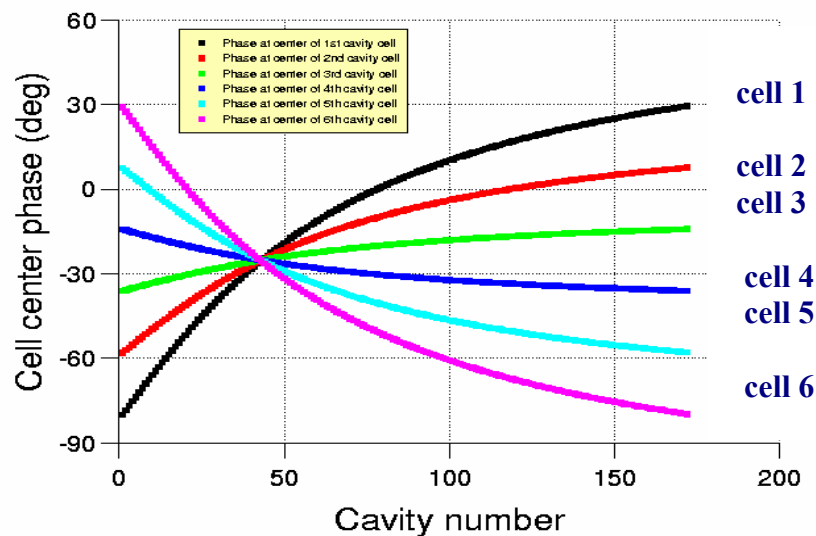


Figure 1.5.2.1: Phase slip of the bunch centre in each of the six cells for the 172 SC cavities: The phase is always between $\pm 90^\circ$, which means energy gain each cell and therefore stable synchrotron oscillations

For a matched 6d Gaussian “control” beam as input to the SC linac and in the absence of RF field errors, very little filamentation is seen at 1334 MeV and the energy spread at the ring injection point, 71 m behind the BR cavity, is limited to ± 0.5 MeV, only a quarter of the ± 2 MeV constraint for loss free ring injection, see Figure 1.5.2.2. Transverse & longitudinal r.m.s. emittances at 400 MeV are assumed to be 20 % larger than those at 20 MeV. Energy spread reduction is obtained by placing warm $\beta = 0.912$ CCL structures 78 m downstream the SC linac, delivering a 13 MV rotation voltage to the beam, see Fig 1.3.1. About 1.45 MW peak RF power are required, see Table 1.4.2. Energy ramping by 4 MeV is done by slowly changing the phase by 18° and increasing the RF power by about 70% during each 0.48 msec pulse.

Using NC cavities for a bunch rotation/energy ramping system is a well known technique, but in principle also SC cavities can be considered. SC structures at 1120 MHz needs only half the voltage, but requires sophisticated RF control: about 100kW peak power is needed to get a short filling time and large bandwidth. The RF generator power has to be reduced to 25 % afterwards to keep the voltage unchanged for bunch rotation, where the beam energy is unchanged. Amplitude and phase of the RF generator has to be slowly changed during each ring pulse in order to get 4 MeV/460 kW increase in energy/power of the LP beam.

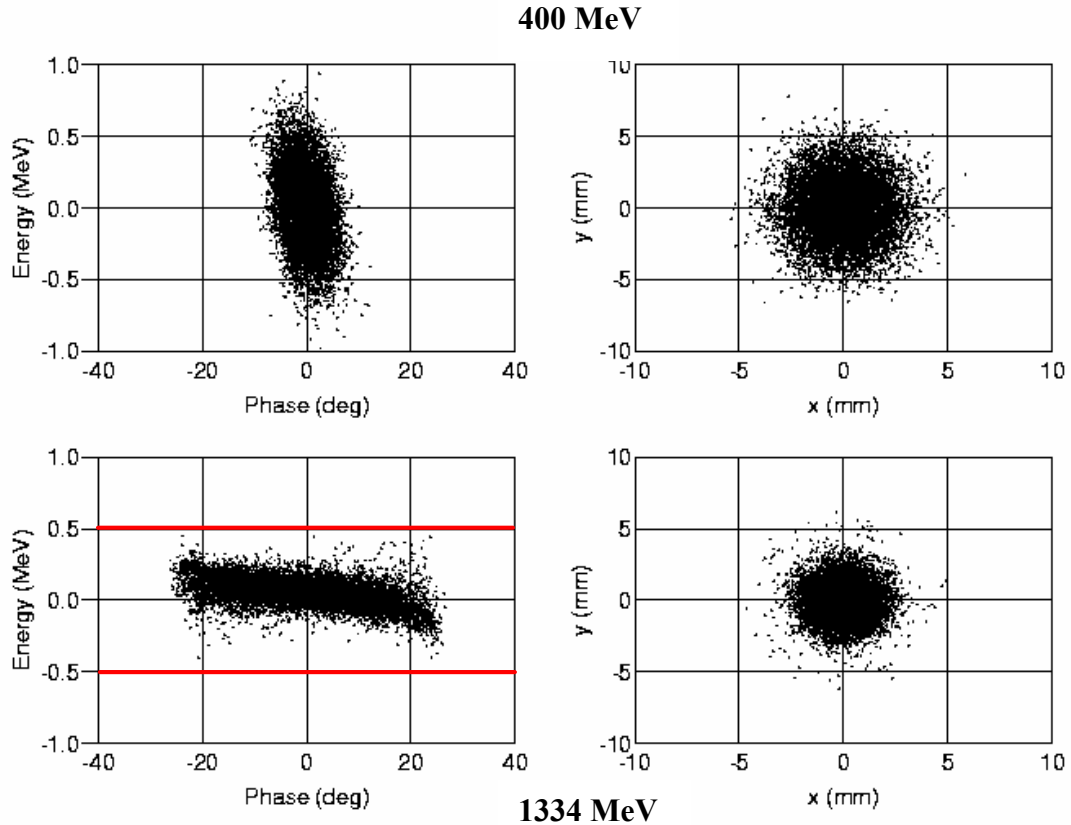


Figure 1.5.2.2: Longitudinal phase space & beam radii along the ESS linac at 400 MeV input (1.row) and at 1334 MeV ring injection point (2.row) for a matched 6d Gaussian “control “ beam and without errors : **No particles are outside ± 0.5 MeV**

As accumulated errors in the NC part of the ESS linac leads to mismatch and phase space filamentation at injection into the SC part, we carefully checked the design of the 228 mA SC linac to be insensitive against strong initial mismatch and different input distributions. As an example we excited a pure “low“ mode (radial by + 15 %, axial by –30 % change in initial radii) at 400 MeV for a 6d Gaussian “ control “ beam in an error free SC linac. As shown in Figure 1.5.2.3, both radii are oscillating out of phase with the bunch length (r.m.s. phase width), as expected [Letchford, 1999]. The beam has reached its final energy after 172 SC cells, but the particle tracking is continued to the BR position (cell 220) up to the ring injection (cell 264). In phase oscillations of the transverse beam radii are visible all along the linac and up to ring injection. The beam is kept transversely focused.

The resulting phase space and radii plots are shown in Figure 1.5.2.4, showing much larger axial than radial filamentation compared to the matched case of Figure 1.5.2.2. This is as predicted for the “low“ mode excitation, as at input only longitudinal halo particles can be in resonance with the oscillating beam core [Letchford, 1999]. The energy spread at the ring injection point is limited to ± 1 MeV, still only half of the ± 2 MeV constraint for loss free ring injection. Exciting the “low” mode or another bunched beam eigenmode [Letchford, 1999] for a 6d Waterbag instead of a Gaussian beam at 400 MeV leads to almost the **same** phase space plots at ring injection, indicating the insensitive of the 228 mA ESS design against details of the input distribution.

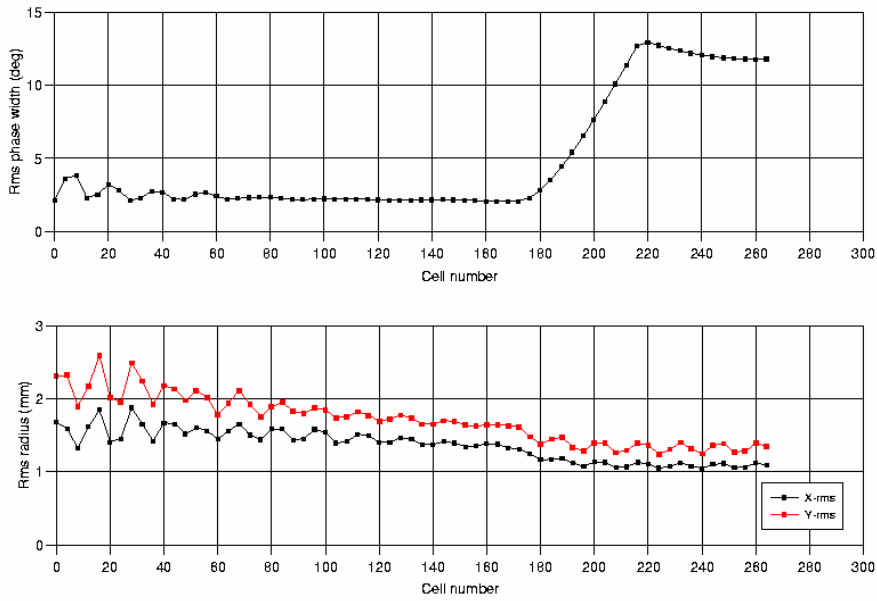


Figure 1.5.2.3: Excitation of a pure “low” mode (radial by + 15 %, axial by –30 % change in initial radii) at 400 MeV for a 6d Gaussian “control” beam: radii and phase width are oscillating up to 52 cell or 600 MeV

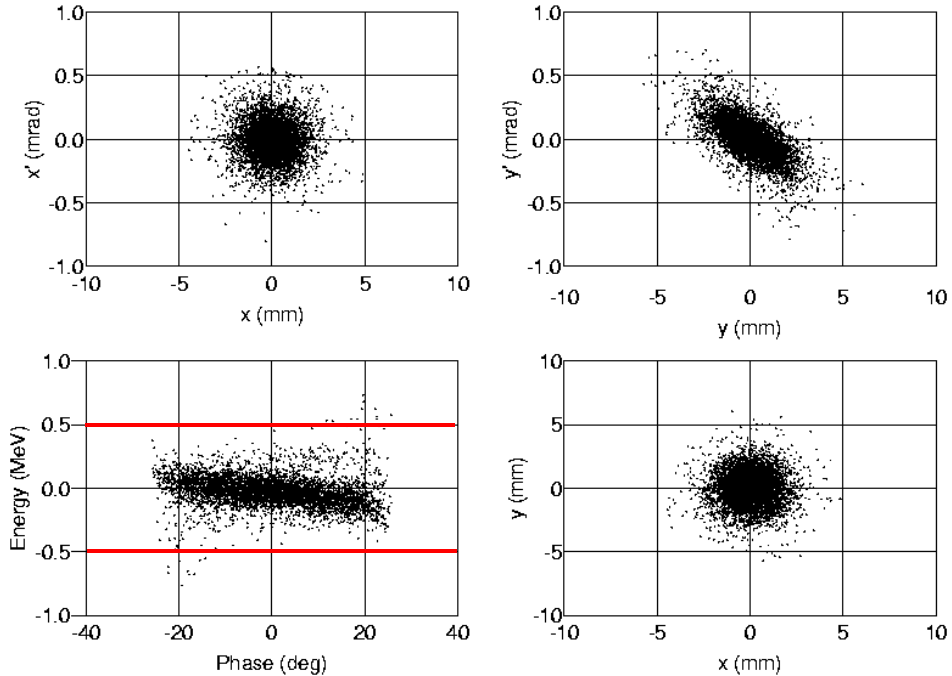


Figure 1.5.2.4: Phase Space plots & beam radii at 1334 MeV ring injection point : longitudinal filamentation is caused by exciting a pure “ low ” mode at 400 MeV: about 10^{-3} particles are outside ± 0.5 MeV

RF field errors along the ESS linac will lead to a shift of the beam centre in energy and phase/time, possibly leading to unacceptable large energy shifts after final bunch rotation. Assuming $\pm 1\%$, $\pm 1^\circ$ RF amplitude and phase errors in each SC cavity, randomly distributed along the 172 SC cavities, and applying the same bunch rotation voltage as used for the Gaussian “control” beam, the bunch centre is displaced by more than ± 1.0 MeV after bunch rotation in about 1 in 10^3 cases, see Figure 1.5.2.5. The input at 400 MeV of $\pm 4.5^\circ$ (1120 MHz) phase resp. & ± 1.3 MeV energy deviation of the beam centre from accumulated RF errors in the preceding warm structures is about 10 times **larger** than obtained after the DTL at 20 MeV [Gerigk, 2003/2].

Even including filamentation due to mismatch and shift of the bunch centre due to accumulated RF amplitude and phase errors in the NC and SC structures, there are less than 1 in 10^4 particles outside ± 2 MeV. The ESS reference linac can tolerate twice as large RF errors in the SC cavities as SNS. Transverse beam core fluctuations due to pulsed RF errors are visible in the LP target beam line, see Figure 1.5.2.3.

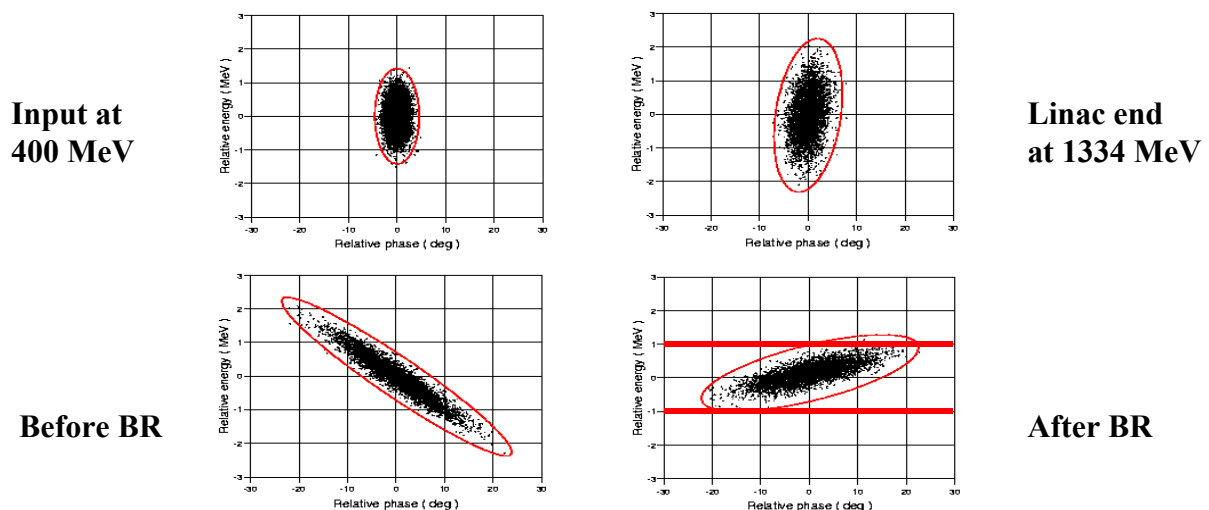


Figure 1.5.2.5: Scatter plots along the ESS SC linac: The red curves represent the 10^{-3} error boundary, increased by more than factor 2 due to $\pm 1\%$ phase resp. $\pm 1^\circ$ RF errors in the SC cavities. After BR, in about 1 in 10^3 cases the beam centre is displaced by more than ± 1.0 MeV

1.4.6 RF control of the pulsed ESS SC cavities

To achieve $\pm 1\%$, $\pm 1^\circ$ RF amplitude and phase errors in each SC cavity during the mismatched 1 msec short pulse, the matched 2 msec long pulse requires a quite sophisticated RF control and an appropriate frequency detuning of each SC cavity. About 30 % RF control power is assumed for the matched LP beam and about 40 % for the mismatched SP. High power results from the 1st SNS medium β cryomodule indicate about ± 40 Hz frequency

oscillations during a 1 msec RF pulse at 10 MV/m accelerating gradient even when using cold piezoelectric tuners [White, 2002]. Much less frequency detuning is observed either at a low power SC test-stand or by using warm piezoelectric tuners [Simrock, 2002].

Detailed numerical simulations with realistic hardware components [Kwon, 2002] and including higher order mode excitations [Ouchi, 2000] are planned to support experimental results from a high priority ESS SC test-stand with a complete 1120 MHz cryomodule and one full power klystron.

The ESS SC linac can tolerate twice as large RF errors as the SNS linac but has a much more demanding RF pulse structure, which cannot be easily simulated even on high power test-stands as we are limited in approximating the different ESS SP& LP beam loading conditions. The chosen frequency of 1120 MHz results in a large cavity bandwidth and reduces Lorentz force frequency detuning. Different methods for stiffening the 1120 MHz ESS SC cavities are under investigations. As the ESS facility is expected to be delayed by a few years, we can profit quite a lot from the ongoing SNS and J-PARC results and from 1300 MHz SC main coupler developments.

1.5 ALTERNATE ESS SCENARIOS

The ESS facility is designed to deliver 5 MW beam power to both the SP and the LP target stations, which leads to unprecedented performance with virtually no compromises for any of the scientific fields in neutron science. On the other hand, using a 16 2/3 Hz LP target station only but with 10 MW beam power at 2 msec, many of the high priority instruments will profit [Mezei, 2003, ESFRI, 2003]. Such an alternative ESS scenario would lead to substantially reduced capital and operating costs: the accumulator rings would not be needed, an H⁺ beam could be used instead of an H⁻ beam, no chopper line is needed and the duty cycle (d.c.) would be low – all points facilitating a high intensity accelerator.

The layout of a basic ESS LP linac is shown in Figure 1.6.1, which is very similar to the ESS SC reference linac design. Two 75 mA H⁺ beams are combined together at 20 MeV and accelerated by 1120 MHz SC cavities up to 3 GeV. Only one type of cryostat is required, as the SC cavity length itself is kept constant, but the number of cells per cavity is changed at 1.4 GeV in order to shorten the SC linac length. An accelerating gradient of 10 MV/m leads to 1.2 MW peak power in the SC main coupler, feasible due to the less than 4 % RF d.c. Simpler and more cost effective HVPS can be used as the beam current is unchanged from pulse to pulse. All accelerator components will profit from the reduced d.c.: only 10 MW wall plug power is needed to achieve 2 MW beam power (2 msec long pulse with 150 mA current) at 400 MeV in the NC structures. To handle somewhat higher beam current is expected to be feasible. The large SC cavity bandwidth of ± 2.6 kHz for a 150 mA beam helps to simplify the RF control system.

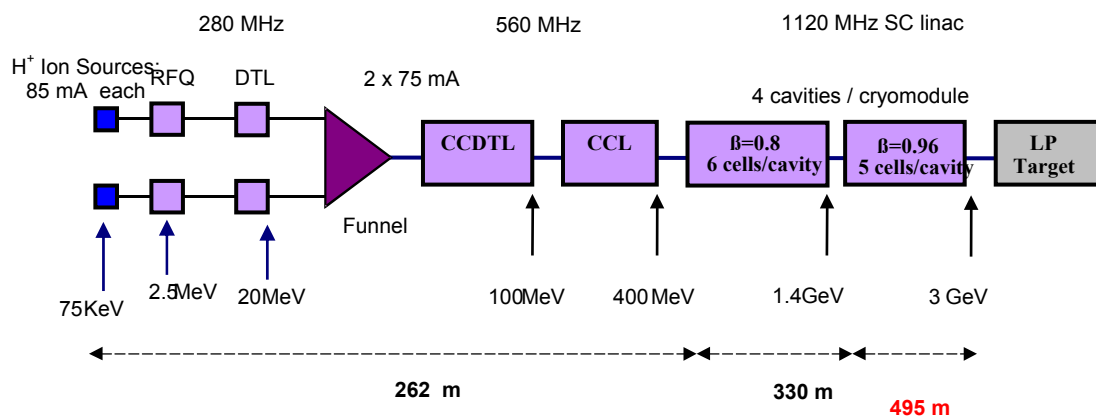


Figure 1.6.1: Layout of a 3 GeV ESS H⁺ linac with 15 MW beam power

The neutron performance of an ESS LP facility can be increased either by going to shorter than 2 msec pulse length or by increasing the average beam power [Mezei, 2003, ESFRI, 2003]. Limiting the final linac energy to 3 GeV due to capital cost reasons leads to the LP facility comparison shown in Table 1.6.1.

An advanced 2 ms ESS LP facility with 15 MW beam power at 3 GeV looks very cost attractive compared to the ESS reference facility and if the novel instrumentation ideas forwarded by the instrument groups can be realised, this would lead to a solution, which for all the presently identified high priority instruments would equal or in most instances be even better than the Bonn proposal, see chapter 5.7. However implications on the target/moderator side need carefully to be evaluated.

Table 1.6.1: Comparison of different ESS LP options

	Basic linac	Extended linac	Advanced linac
Average power	10 MW	10 MW	15 MW
Final energy	2 GeV	3 GeV	3 GeV
Pulse length	2 msec	1.34 msec	2 msec
SC linac length/m	524: 330 & 194	825 : 330 & 495	825 : 330 & 495
power/ SC coupler	46 kW	33 kW	46 kW
AC cryo power	4 MW	6 MW	6.5 MW

Studies are necessary to find the acceptable RF error limits in the SC cavities which will lead to transverse beam core fluctuations in the target beam line. The large SC cavity bandwidth helps to simplify the pulsed RF control system.

To accelerate a 150 mA H⁺ beam in SC cavities at lower frequencies is limited by the peak power capability of the SC main coupler and will require much more AC cryo-power. The pulsed RF control is more demanding as the SC cavity bandwidth is smaller.

1.6 STATUS OF THE ESS ACCELERATOR SYSTEM – THE WAY AHEAD

To have a decision on the ESS in 4-5 years time requires a project following the proposed time schedule associated by competence centres to look into key technological questions. The ESS linear accelerator needs two dedicated test-stands for prototyping and development: a 2.5 MeV chopping line as test-bed for front end components and a complete 1120 MHz cryo-module as full power test-bed for SC couplers.

1.7 ACKNOWLEDGEMENTS

This short summary for the new ESS SC reference linac is based on the considerable work of many colleagues in the last 6 months. Without all these contributions it would have been impossible to describe the ESS SC reference linac as it is up to now.

REFERENCES

- [Billen, 2002] J H Billen, L M Young
Poisson Superfish V6, Los Alamos National Laboratory, LA-UR-96-1834, 2002
- [Bothe, 1996] W Bothe
Dual Mode Pulse Generation for ESS, ESS report 96-40-L, April 1996
- [Bourque, 2000] R Bourque, G Laughon,
Proc. PAC 2001, Chicago, USA, p 1083
- [Clarke-Gayther, 2002] M A Clark-Gayther et al
Proc. EPAC 2002, Paris, France, p 2133 & p 2136
- [Clausen, 2003] K N Clausen
Proc. ICANS –XVI, Düsseldorf-Neuss, May 2003, p 61, and
ESS newsletter volume 1 May 2003 in
http://neutron.neutron-eu.net/FILES/ess_news1-may03.pdf
- [ERL project] Energy Recovery Linac (ERL) Project at Cornell University
<http://erl.chess.cornell.edu>
- [ESFRI 2003] Medium to Long-Term Future Scenarios For Neutron-Based Science
In Europe, Working Group on Neutron Facilities European Strategy
Forum on Research Infrastructures, 2003,
http://www.neutron-eu.net/en/files/esfri_report.pdf
- [ESS, 2002] The ESS Project Volume III – Technical Report,
<http://www.neutron-eu.net> ISBN 3-89336-303-3, 2002, 438 pages

- [Gerigk, 2003/1] F Gerigk
Revised ESS Front-End, (2.5 – 20 MeV), internal ESS note ESS 03-138-A, December 2003
- [Gerigk, 2003/2] F Gerigk
Halo Studies for the ESS Linac and Front-Ends, Halo03, Long Island, 2003
- [Gobin, 2002] R Gobin et al
Proc. EPAC 2002, Paris, France, p 1715
- [Kwon, 2002] S Kwon, A Regan, Yi M Wang
NIM A 482, 2002, p12
- [Letchford, 1999] A Letchford, M Pabst, K Bongardt
Proc. PAC 1999, New York, USA, p1767
- [Mezei, 2003] F Mezei
Proc. ICANS–XVI, Düsseldorf-Neuss, May 2003, p135
- [Ouchi, 2000] N Ouchi et al
Proc. LINAC 2000, Monterey, USA, WE205
- [Oyama, 2003] Y Oyama
Proc. ICANS–XVI, Düsseldorf-Neuss, May 2003, p.7 and
<http://j-parc.jp/>
- [Pabst, 2002] M Pabst, K Bongardt
Proc. LINAC 2002, Gyeongju, Korea, TU436
- [Pabst, 2003] M Pabst, K Bongardt
Beam Dynamics in the 1120 MHz ESS SC Linac, internal ESS report 03-163-L, December 2003
- [Qiang, 2000] J Qiang, R D Ryne, S Habib, V Decyk
Journal of Computational Physics 163, 2000, p 1
- [Sherman, 2002] J D Sherman et al
Proc. EPAC 2002, Paris, France, p 284
- [Simrock 2002] S N Simrock
Proc. LINAC 2002, Gyeongju, Korea, WE204
- [SNS project] <http://www.sns.gov/>
- [TESLA project] TESLA Technical Design Report, <http://tesla.desy.de>
- [Thomason, 2002] J W G Thomason, R Sidlow, M O Whitehead
Rev. Sci. Instruments 73(2), 2002, p 896

- [Uriot] this SUPERFISH version is provided by D Uriot, CEA Saclay
- [Volk, 1998] K Volk, A Maaser, H Klein
Proc. LINAC 1998, Chicago, USA, p 896
- [White, 2002] M White et al
Proc.LINAC 2002, Gyeongju, Korea, MO101, and I E Campisi et al,
Proc. LINAC 2002, Gyeongju, Korea, TU476
- [Yoshino, 2000] K Yoshino et al,
Proc. LINAC 2000, Monterey, USA, TUD1